Monitoring changes of cellular metabolism and microviscosity *in vitro* based on time-resolved endogenous fluorescence and its anisotropy decay dynamics

Wei Zheng
Dong Li
Jianan Y. Qu
Hong Kong University of Science and Technology
Department of Electronic and Computer Engineering
Clear Water Bay, Kowloon
Hong Kong, China

Abstract. Reduced nicotinamide adenine dinucleotide (NADH) is a well-known metabolic coenzyme and endogenous fluorophore. In this study, we develop a system that simultaneously measures time- and wavelength-resolved fluorescence to extract free and protein-bound NADH signals from total cellular fluorescence. We analyze temporal characteristics of NADH fluorescence in a mixture of NADH and lactate dehydrogenase (LDH) as well as in living cell samples. The results show that in both the NADH/LDH mixture and cell samples, a fraction of free NADH and protein-bound components can be identified. The extracted free and bound NADH signals are confirmed by time-resolved measurement of anisotropy decay of NADH fluorescence, based on the fact that free NADH is a small fluorescent molecule with much shorter rotational diffusion time than bound NADH. The ratio of free NADH signal to bound NADH signal is very different between normal and cancer cervical epithelial cells. In addition, the ratio changes significantly when the cell samples are treated with a mitochondrial inhibitor or uncoupler, demonstrating that the method is sensitive to monitor cellular metabolic activity. Finally, we demonstrate that the microviscosity for relatively small molecules such as NADH in cells could be extracted from wavelength- and time-resolved NADH fluorescence of living cell samples.
[DOI: 10.1117/1.3449577]

Keywords: fluorescence spectroscopy; nicotinamide adenine dinucleotide; endogenous fluorophores; fluorescence lifetime; anisotropy decay; global fitting.

Paper 09393RRR received Sep. 2, 2009; revised manuscript received Apr. 23, 2010; accepted for publication Apr. 26, 2010; published online Jun. 15, 2010.

1 Introduction

Reduced nicotinamide adenine dinucleotide (NADH) is a principal electron donor in cellular energy metabolism.[1] Since NADH is an endogenous fluorescent molecule, extensive research has been focused on its fluorescence as a noninvasive probe of a cell's metabolic state.[2–5] Intracellular NADH exists in two forms, one is free and the other is bound to many different dehydrogenases. Previous thermodynamic studies revealed that the activity of a dehydrogenase depends on the concentration of free NADH.[3] Furthermore, it was found that free NADH can play active or restrictive roles, even binding to the same dehydrogenase.[6] In living cells, the free and bound forms of NADH exist in a dynamic equilibrium, and the free NADH functions after binding to dehydrogenases in energy metabolism. Therefore, the ratio of these two forms of NADH could indicate the metabolic state of a cell.[5,7] Although the definition of a redox state is based on the measurement of NADH and NAD+, because NAD+ does not emit fluorescence, considerable attention has been paid to determine the redox state by measuring the fraction of intracellular free and bound NADH.

The fluorescence lifetime, which probes the time that a molecule remains in its excited state before decaying back to the ground state, is a sensitive method to probe free and bound NADH.[8] Previous studies revealed that cellular NADH fluorescence consists of short- and long-lifetime components.[4,5] The long-lifetime component comes from protein-bound NADH, while the short-lifetime component is a mixture of free and bound NADH, because fluorescence decay of bound NADH is usually multiexponential with the lifetime component(s) comparable with that of free NADH.[5,9,10] It is thus difficult to attribute the short lifetime component to the free or bound NADH. Time-resolved measurement of fluorescence anisotropy targets the rotational mobility of a fluorophore based on the polarization of the fluorescence. It

Address all correspondence to: Jianan Y. Qu, Department of Electronic and Computer Engineering, Hong Kong University of Science and Technology, Clear Water Bay, Kowloon, Hong Kong. Tel: (852) 2358-8541; Fax: (852) 2358-1485; E-mail: eequ@ust.hk

1083-3668/2010/15(3)/037013/11/$25.00 © 2010 SPIE

offers the sensitive means to distinguish between free and bound NADH due to their large differences in molecular size. In particular, the method developed by Vishwasrao et al. in 2005 set elegant framework for extraction information on cellular metabolism from fluorescence anisotropy measurements.[11] They reported that changes in intracellular NADH concentration can be measured, and that these changes have been underestimated using traditional time-resolved fluorescence spectroscopy. In this study, we developed a time- and wavelength-resolved system to measure the fluorescence signals, and used a global-fitting method to analyze the fluorescence intensity and anisotropy decay dynamics at 16 (12 for cells) wavelength bands. The technique improved the accuracy of fitting analysis for the extraction of the information on cellular metabolism. In addition, we demonstrated that cellular viscosity could be measured as well.

Cellular viscosity is another important biological parameter that determines the transports of small organic and inorganic solutes, macromolecules, and other cellular organelles in living cells.[12,13] Cellular viscosity impacts a number of dynamic intracellular processes. For example, the diffusion of small solutes is relevant to metabolite uptake and second messenger signaling. The cell development and division are controlled by the transports of proteins and DNA in cytoplasm. Furthermore, the diffusion of DNA is important in antisense and gene therapy.[14] Several techniques based on the magnetic resonance method, fluorescence recovery after photobleaching (FRAP), fluorescence correlation spectroscopy (FCS), and time-resolved fluorescence anisotropy have been developed to measure cellular viscosity.[15–19] However, all of these methods need to use extrinsic labels, such as magnetic particles, spin label probes, and exogenous fluorophores. A noninvasive approach based on the endogenous signal of a cell that does not create a disturbance to the cellular environment is a more desirable technique for the measurement of cellular viscosity. In this study, we developed a time- and wavelength-resolved fluorescence spectroscopic technique to analyze NADH signals in cells. The free NADH and protein-bound NADH signals were used as endogenous probes to detect the cellular metabolism and microviscosity from relatively small organic and inorganic solutes in a cell simultaneously.

2 Materials and Methods

2.1 *Decay of Fluorescence Intensity and Its Associated Anisotropy*

The time- and wavelength-resolved fluorescence spectroscopy system used in this study measures two orthogonal polarization components of fluorescence from samples. They are parallel (I_p) and perpendicular (I_s) with respect to the polarization of the excitation light. With these two components, the total fluorescence intensity decay and fluorescence anisotropy decay can be calculated by the following equations, respectively:[11,20]

$$I(t) = I_p(t) + 2GI_s(t), \tag{1}$$

$$r(t) = \frac{I_p(t) - GI_s(t)}{I_p(t) + 2GI_s(t)}, \tag{2}$$

where the G factor describes the sensitivity of the optics and the detector to polarization. In this study, we used a tungsten lamp as an isotropic emission source to determine the G factor of our fluorescence measurement system.

Fluorescence intensity decay can be fitted by the following equation,

$$I_\lambda(t) = \left[\sum_{i=1}^{n} a_{\lambda,i} \cdot \exp\left(-\frac{t}{\tau_{\lambda,i}}\right)\right] \otimes R_\lambda(t), \tag{3}$$

where $R_\lambda(t)$ is the temporal response of the system, and $\tau_{\lambda,i}$ and $a_{\lambda,i}$ are the fluorescence lifetime and pre-exponential amplitude of the i'th term at λ wavelength, respectively. Based on these fitting parameters, some useful quantities can be deduced as follows.[5,11]

The intensity fraction of each term in the total fluorescence:

$$f_{\lambda,i} = \frac{a_{\lambda,i}\tau_{\lambda,i}}{\sum_{i=1}^{n} a_{\lambda,i}\tau_{\lambda,i}}, \tag{4}$$

and the decay-associated spectrum (DAS),

$$S_i(\lambda) = a_i(\lambda)\tau_i(\lambda). \tag{5}$$

In this study, free and protein-bound NADH are regarded as different fluorophores, with each having its own distinct intensity and anisotropy decay. When there are two or more different fluorophores in the sample, the measured anisotropy decay is an average of the anisotropy weighted by its intensity fraction. The fluorescence associated anisotropy in Eq. (2) is then determined by the following equation:[11,20]

$$r_\lambda(t) = \frac{D_\lambda(t)}{I_\lambda(t)} = \frac{\left[\sum_{i=1}^{n} a_{\lambda,i}\exp\left(-\frac{t}{\tau_{\lambda,i}}\right) r_{\lambda,0i}\exp\left(-\frac{t}{\theta_{\lambda,i}}\right)\right] \otimes R_\lambda(t)}{\left[\sum_{i=1}^{n} a_{\lambda,i}\exp\left(-\frac{t}{\tau_{\lambda,i}}\right)\right] \otimes R_\lambda(t)}, \tag{6}$$

where $r_{\lambda,0i}$ and $\theta_{\lambda,i}$ are the initial anisotropy and the rotational diffusion time of the i'th fluorophore at the λ wavelength, and $D_\lambda(t)$ is the difference between two orthogonal polarization components of fluorescence, as defined in Eq. (2).

In practice, we fit the denominator,

$$I_\lambda(t) = \left[\sum_{i=1}^{n} a_{\lambda,i}\exp\left(-\frac{t}{\tau_{\lambda,i}}\right)\right] \otimes R_\lambda(t),$$

and the numerator,

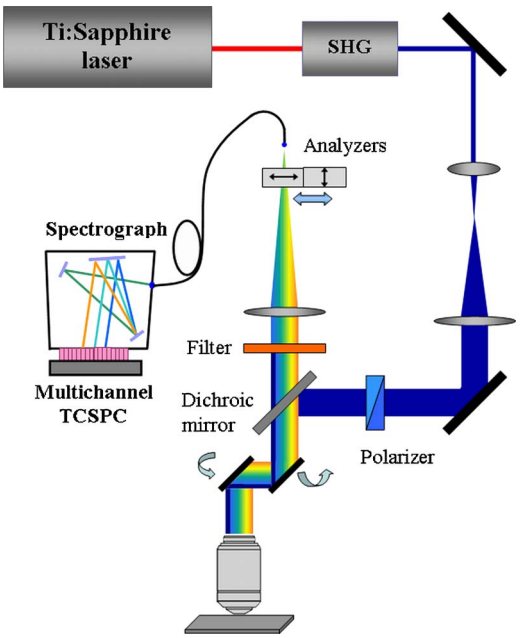

Fig. 1 Schematic diagram of time- and wavelength—resolved fluorescence system.

$$D_\lambda(t) = \left[\sum_{i=1}^{n} a_{\lambda,i} \exp\left(-\frac{t}{\tau_{\lambda,i}}\right) r_{\lambda,0i} \exp\left(-\frac{t}{\theta_{\lambda,i}}\right)\right] \otimes R_\lambda(t),$$

separately, because $I_\lambda(t)$ only fits the experimentally measured decay of fluorescence intensity $I(t)$ in Eq. (1). From the results of the fitting of the denominator, we obtain the parameters ($\tau_{\lambda,i}$ and $a_{\lambda,i}$) that provide information on free NADH of short-lifetime fluorescence and protein-bound NADH of long-lifetime fluorescence. These parameters are held constant in the fitting of $D_\lambda(t)$ to the measured $D(t)=r(t)\times I(t)$ to determine the initial anisotropy and rotational diffusion time, which are $r_{\lambda,0i}$ and $\theta_{\lambda,i}$, respectively. Finally, the analytical description of anisotropy decay is obtained from Eq. (6). In the fitting of $I_\lambda(t)$ and $D_\lambda(t)$, the residual χ^2 for the minimum search algorithm is defined in Refs. 11 and 20. All custom-written fitting programs used in this study are based on the Marquardt-Levenberg nonlinear least-squares algorithm and written in MatLab (MathWorks, Natick, Massachusetts).

2.2 *Experimental Setup and Sample Preparation*

A schematic diagram of the time- and wavelength resolved fluorescence spectroscopy system is shown in Fig. 1. The setup was based on a confocal system equipped with a polarizer in the excitation path and a pair of analyzers in the emission path. Briefly, the second-harmonic generation (SHG) of a femtosecond Ti:sapphire laser provided 360-nm excitation, nearly to the excitation peak of NADH fluorescence. This ensured that the excited cellular fluorescence was dominated by NADH signal.[21,22] The expanded laser beam was polarized by a Glan-Taylor prism (Melles Griot 03PTA403) placed before a dichroic mirror. An objective lens (Leica 40×, NA 0.75) focused the beam into the sample and collected the backscatter fluorescence signals. The excitation power on the sample is about 10 μW. To reduce the possibility of photobleaching in samples, the laser focus was scanned over a 100×100-μm sampling area by a pair of galvo-mirror scanners, and the recorded signal was the integration of fluorescence over the sampling area.[5] We found that photobleaching could be negligible, because the cellular autofluorescence spectra and time-decay remained the same after multiple scanning over the sampling area. The previous study demonstrated that the fluorescence signals integrated over the sampling area in living cell samples were dominated by the NADH fluorescence from mitochondria.[23]

A 400-μm optical fiber was used as a pinhole to collect the confocal fluorescence and to conduct the signals to a spectrograph. A grating with a blaze wavelength at 400 nm was used in the spectrograph. The detector of the spectrograph was a linear array of photomultiplier tubes (PMTs) connected with a time-correlated single photon counting (TCSPC) module to record time-resolved fluorescence signals in 16 consecutive spectral bands from 420 to 520 nm at 6.2-nm intervals. Two orthogonal analyzers driven by a computer-controlled switcher were placed before the fiber. The orientation of each analyzer was adjusted carefully according to the polarization of the excitation beam. The parallel and perpendicular components of the time-resolved fluorescence emission, $I_p(t)$ and $I_s(t)$ were measured sequentially for equal amounts of exposure time of 60 s. The temporal response function of each wavelength channel $R_\lambda(t)$ was measured for accurate fitting of multiexponential decay of NADH fluorescence. In this study, the fluorescence of 2-[4-(dimethylamino)styryl]-1-methylpyridinium iodide (DASPI) dissolved in ethanol was used to measure the temporal response function of the system, since its fluorescence lifetime is significantly shorter than the response of TCSPC-based detection[24,25] and the responses of all the channels can be measured simultaneously. The spectral response of the system was calibrated by using a NIST-traceable tungsten light source [Ocean Optics (Dunedin, Florida) LS-1-CAL]. To test the performance of the system, we measured the time-resolved fluorescence of rhodamine 6G in ethanol and rose bengal in methanol, the well-known fluorescent dyes. After deconvolution of the system temporal response, the fluorescence lifetimes of rhodamine 6G in ethanol and rose bengal in methanol were 3.77 and 0.51 ns, respectively. The results are very consistent with those in the published literature.[26,27]

A variety of NADH solutions and living cell cultures were used as samples in this study. To study the effects of cellular enzyme on the decays of NADH fluorescence intensity and anisotropy, pure NADH solution and the mixture solutions of NADH and lactate dehydrogenase (LDH), an enzyme present in a wide variety of organisms in living cells, were prepared for time- and wavelength-resolved fluorescence measurements. NADH powder and LDH solution were purchased from Sigma-Aldrich (Saint Louis, Missouri). The NADH solution was freshly prepared in 10-mM tris(hydroxymethyl)aminomethane (Tris) buffer at pH 8. In the experiments, the 1000-unit/ml LDH solution was mixed in a 1:1 volume with the NADH solution. NADH concentration in the mixture was 500 μM.

SiHa and Ect1 cell lines were provided from the American Type Culture Collection (ATCC). The SiHa cell line was established from cervical cancer tissue, whereas the Ect1 cell

line was developed from normal cervical tissue. SiHa cells were grown in Dulbecco's Modified Eagle Medium (DMEM) containing 10% fetal bovine serum, and Ect1 cells were cultured in Keratinocyte-Serum-Free medium with 0.1-ng/ml human recombinant EGF and 0.05-mg/ml bovine pituitary extract. The cells were maintained in a 5% CO_2 incubator at 37 °C and cultured every 4 to 5 days. On the day before the measurements, the cells were trypsinized from culture dishes and grown on microscope coverslips. Before the measurements, the cells were washed with phosphate buffered saline (PBS) solution twice to eliminate the fluorescence of the medium. The confluence of monolayer cells in the measurements was about 90%.

To disturb the redox potential of the cells, 5-mM sodium cyanide (NaCN) and 100-μM carbonyl cyanide 3-chloro phenylhydrazone (CCCP) were used. NaCN affects the mitochondrial transport by blocking the transfer of electrons from the electron donors, so the oxidation of NADH is prohibited and the free NADH is accumulated. CCCP reduces the proton gradient and thus increases particle exchange across the mitochondrial membrane. Free NADH in mitochondria is released to the cytosol and rapidly oxidized.[28] In this study, cell cultures were treated with NaCN or CCCP solution for five minutes then measured in PBS.[5]

2.3 *Global Fitting Analysis*

The global analysis method described in Ref. 29 was used to fit Eq. (6) and obtain the parameters related to cellular metabolism and viscosity. Briefly, a vector **g**, including all the shared parameters and the independent parameters, was created. For example, rotational diffusion time and fluorescence lifetime in this study are independent of emission wavelength and considered the shared parameters. The rotational diffusion time reflects the rotational mobility of a fluorophore, which depends on its shape, size, or flexibility. The fluorescence lifetime indicates the dwell time of the electron in the lowest vibrational level of the excited state, and it is generally independent of emission wavelength.[20] We have measured the fluorescence lifetimes of several fluorophores, such as aqueous NADH, the mixture of LDH and NADH, rhodamine 6G, etc., and found that the lifetimes are all independent of the emission wavelength. However, the pre-exponential amplitudes at each wavelength are considered independent parameters, because they are a function of the fluorophore's concentration and spectral line shape. Then the **g**-vector and the initial testing value of each fitting parameter were used to solve the Marquardt-Levenberg equation. The elements that were related to the shared parameters were processed by each curve, and the independent parameters were only restricted by their own decay curves.[29] The Marquardt-Levenberg nonlinear least-squares algorithm was used to search the global minima for all the curves. The details of the fitting algorithm can be found in Ref. 29.

3 Results and Discussions

3.1 *Analyses of the Measurements from Reduced Nicotinamide Adenine Dinucleotide Solutions*

Since there are folded and unfolded conformations of free NADH in aqueous environments which were first discovered

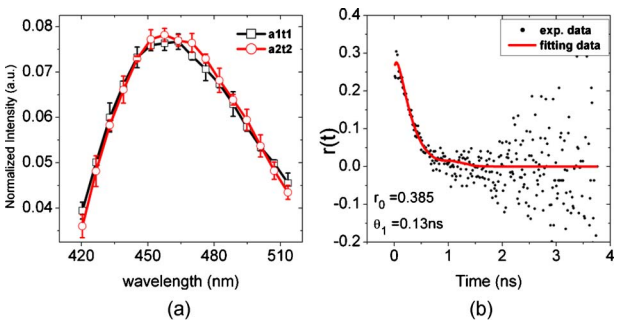

Fig. 2 Results of global fitting analysis of fluorescence signals from pure NADH solution. (a) The normalized decay associated spectra (DAS) of two conformations of aqueous NADH (a biexponential function was used to describe the fluorescence intensity decay curve, and 16 curves at consecutive emission wavelengths were globally analyzed). (b) The measured and fitted fluorescence anisotropy decay.

from x-ray crystallographic data,[30] a biexponential function of Eq. (3) was used to describe the fluorescence intensity decay curves. 16 curves at consecutive emission wavelengths from 420 to 520 nm were globally analyzed by the method described in Sec. 2, where the lifetimes τ_1 and τ_2 are the shared parameters of all curves, and the pre-exponential amplitudes $a_{\lambda,1}$ and $a_{\lambda,2}$, depend on their own curves. Excellent fitting was achieved with $\chi^2 < 2.5$. The measured τ_1 and τ_2 are 0.252 ± 0.004 and 0.583 ± 0.011 ns, respectively. The results agree well with reports in the literature.[30,31] By using the fitting results of lifetimes and pre-exponential amplitudes, the decay-associated spectra (DAS) of the folded and unfolded conformations of NADH were calculated based on Eq. (5). The results are displayed in Fig. 2(a). As can be seen, the spectra of two different conformations of NADH are almost identical. The ratio of pre-exponential amplitudes a_1/a_2, averaged over all 16 channels, is 2.28 ± 0.19. Furthermore, we tested the fitting of free NADH fluorescence using a monoexponential model. The larger χ^2 (>10) indicated that the monoexponential model is not as accurate as the biexponential model in the description of the fluorescence decay of aqueous free NADH.

Next, the fluorescence anisotropy decay of free NADH in an aqueous solution was fitted using Eq. (6) with known parameters of the fluorescence intensity decay (τ_1 and τ_2, $a_{\lambda,1}$, and $a_{\lambda,2}$). A monoexponential function was used to describe fluorescence anisotropy decay based on the assumption that two different conformations of free NADH contribute in the same way to the rotational diffusion of free NADH molecules. Excellent fitting results shown in Fig. 2(b) indicate that a monoexponential function is adequate to describe the fluorescence anisotropy decay of free NADH. The average rotational diffusion time (θ) and the average initial anisotropy (r_o) over the 16 wavelength bands are 0.128 ± 0.004 ns and 0.368 ± 0.029, respectively, which are consistent with the results of previous studies.[30,32]

Analysis of the time-resolved fluorescence anisotropy decay provides information on the rotational mobility of a molecule, and the rotational diffusion time sensitively reflects the volume of the molecule. This relationship is described by the Stokes-Einstein equation $\theta = \eta V/kT$, where η is the viscosity, T is the temperature in Kelvin, k is the Boltzmann constant,

and V is the hydrodynamic volume of the rotating unit.[20] In the measurement, T was controlled at 295 K; the viscosity of water is known as 0.958 cP.[33] As a result, the volume of NADH was found to be about 544 ± 17 Å^3, slightly larger than the previously reported 493 Å^3 that was theoretically calculated by using Van der Waals increments method.[34] The difference may be due to the complementary hydration volume.[30] For simplification, NADH is approximately regarded as spherically shaped molecules in this study.

We mixed LDH with NADH to validate our method for the extraction of free and protein-bound NADH signals. The following formula was used to describe the NADH fluorescence intensity decay:

$$I_\lambda(t) = I_{\lambda\_free}(t) + I_{\lambda\_bound}(t),$$

$$I_{\lambda\_free}(t) = a_f\left[a_{\lambda,1}\exp\left(-\frac{t}{\tau_1}\right) + a_{\lambda,2}\exp\left(-\frac{t}{\tau_2}\right)\right] \otimes R_\lambda(t),$$

$$I_{\lambda\_bound}(t) = \left[\sum_{i=1}^{n} a'_{\lambda,i}\exp\left(-\frac{t}{\tau'_i}\right)\right] \otimes R_\lambda(t). \quad (7)$$

The parameters of free NADH fluorescence (τ_1 and τ_2, $a_{\lambda,1}$ and $a_{\lambda,2}$) are obtained from the measurements of aqueous pure NADH and held as constant. The parameter a_f is proportional to free NADH concentration.

Though bound NADH may have multiple decay channels, it was found that a biexponential model ($n=2$) for the bound-NADH term was adequate to produce accurate fitting ($\chi^2 < 2$) of the time-resolved fluorescence signals measured from NADH and LDH mixtures. When n was greater than 2, multiple local minima led to a series of fitting parameters without physical meaning. As a result, the decay time constants of bound-NADH fluorescence (τ_1 and τ_2), the shared parameters in the global fitting, were found to be 1.03 ± 0.04 and 2.51 ± 0.19 ns, respectively. The average ratio of two pre-exponential amplitudes $a'_{\lambda,1}/a'_{\lambda,2}$ was 2.77 ± 0.11. The χ^2 value was 1.88. Representative fitting results are shown in Fig. 3. As can be seen, the decay-associated spectra of two components of bound-NADH are almost identical and the total fluorescence spectrum of NADH, and the LDH mixture was accurately fitted. The experimentally measured fluorescence intensity decay was also accurately fitted using Eq. (7), as shown in Fig. 3(b). It should be pointed out that the LDH purchased from Sigma-Aldrich was not purified, and only the unit of activity was provided. Therefore, the exact ratio of free to bound NADH in the mixture could not be accurately estimated.

To verify whether the free and bound NADH could be unambiguously distinguished based on Eq. (7), we analyzed the fluorescence anisotropy decay dynamics of the mixture. A typical fluorescence anisotropy decay curve measured from a NADH and LDH mixture is shown in Fig. 3(c). Unlike the result of aqueous NADH shown in Fig. 2(b), the anisotropy decay curve exhibited a quick decrease at first, followed by a small increase and then slow decay at longer times. This is a typical pattern of associated anisotropy decay with two fluorophores of different intensity and anisotropy decays in the mixture.[11,20] The fluorescence intensity decay of free NADH was quicker than that of bound NADH; its fractional intensity decreased progressively. As a result, the dominant contribution to the total anisotropy decay curve changed from free NADH at the start to bound NADH at the end. The associated anisotropy curve was fitted by the global analysis program using the following model based on the definition of $D_\lambda(t)$ in Eq. (6), as described in Sec. 2.1,

$$D_\lambda(t) = \left[I_f^{\mathrm{NADH}}(t)\cdot r_{\lambda,01}\exp\left(-\frac{t}{\theta_1}\right) + \sum_{i=1}^{2} a'_{\lambda,i}\exp\left(-\frac{t}{\tau'_i}\right)\cdot r'_{\lambda,i}\cdot\exp\left(\frac{t}{\theta_2}\right)\right] \otimes R_\lambda(t),$$

$$I_f^{\mathrm{NADH}}(t) = a_f\left[a_{\lambda,1}\exp\left(-\frac{t}{\tau_1}\right) + a_{\lambda,2}\exp\left(-\frac{t}{\tau_2}\right)\right],$$

$$I_b^{\mathrm{NADH}}(t) = a'_{\lambda,1}\exp\left(-\frac{t}{\tau'_1}\right) + a'_{\lambda,2}\exp\left(-\frac{t}{\tau'_2}\right),$$

$$I_\lambda(t) = [I_f^{\mathrm{NADH}}(t) + I_b^{\mathrm{NADH}}(t)] \otimes R_\lambda(t), \quad (8)$$

where a and τ are the parameters obtained from the fluorescence intensity decay analysis. In practice, the initial anisotropy of free NADH $r_{\lambda,01}$ was set as the value measured from the aqueous NADH solution. This is a reasonable assumption, because the initial anisotropy of a molecule is determined by the angle between the absorption and emission transition moments.[20]

Again, accurate fitting was achieved as shown in Fig. 3(c). The θ_1 of NADH and LDH mixture is 0.176 ± 0.009 ns, while the change of χ^2 value becomes negligible when θ_2 is greater than 30 ns in the fitting. In fact, accurate measurement of θ_2 longer than 10 ns is impractical because of a limited measurement window determined by the repetition rate of the excitation laser (78 MHz) and the fluorescence intensity decay of bound NADH ($\sim$2 ns). The results demonstrate that fluorescence anisotropy decay of the first term in Eq. (8) is at least two orders shorter that the second term. This provides solid evidence that the first term comes from free NADH and the second term is from bound NADH, because the LDH molecule (27 kDa) is much larger than the NADH molecule (709 Da).

In addition, the rotational diffusion time of free NADH was increased compared with that of aqueous NADH solution. This is not surprising, because the diffusion time is proportional to the viscosity of the environment, and the viscosity of the mixture solution increased when LDH with much greater molecular weight was added. Based on the hydrodynamic volume of aqueous NADH measured previously and the Stokes-Einstein equation $\theta_1 = \eta V/kT$, we obtained the viscosity coefficient of the NADH and LDH mixture at about 1.32 ± 0.06 cP. To verify the results, we measured the viscosity coefficient of the NADH and LDH mixture by using a microchannel viscometer. Details of the technology and measurement procedures were described in Ref. 35. The measured

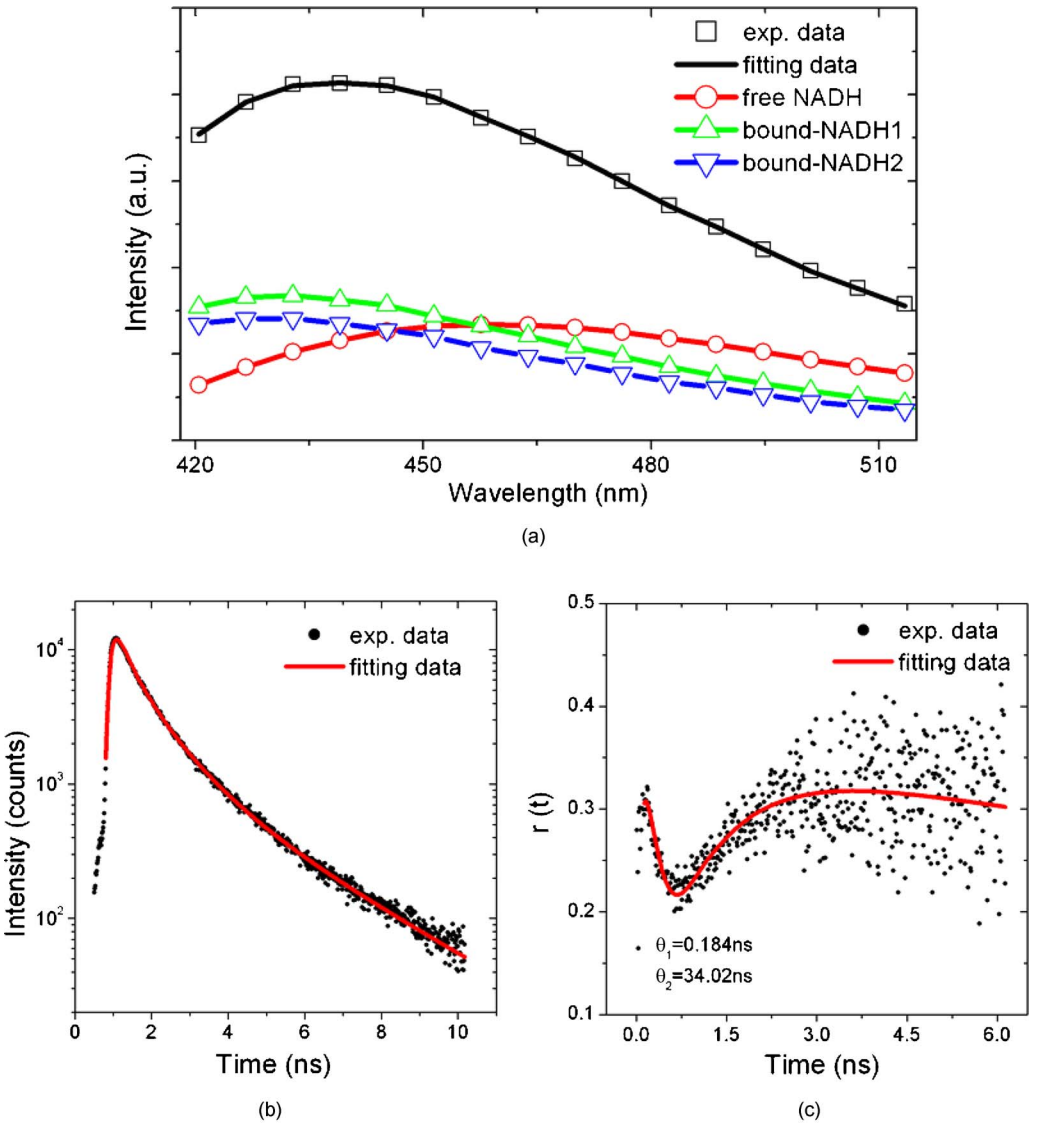

Fig. 3 Representative results of global fitting analysis of fluorescence signals measured from the mixture solution of NADH and LDH. (a) The spectra of the measured and fitted NADH fluorescence signals. Open squares: experimentally measured total spectral signal. Solid line: the fitted total signal. Open circles: fractional decay associated spectrum (DAS) of free NADH. Up-triangles: fractional DAS of bound NADH1. Down-triangles: fractional DAS of bound NADH2. (b) The measured and fitted fluorescence intensity decay. (c) The measured and fitted fluorescence associated anisotropy decay.

viscosity coefficient of 1.34 ± 0.02 cP was consistent with our results based on the analysis of NADH fluorescence anisotropy decay.

3.2 *Analyses of the Measurements from Living Cell Samples*

When a fluorescent molecule presents in a solution of complicated chemical composition, the solvent effect will affect the fluorescence measurements. There are three major mechanisms that can cause changes in spectral and temporal fluorescence characteristics.[20] Binding with other molecules in the solution causes spectral shift, change of fluorescence lifetime, and decrease of mobility. The solvent shell effect shifts fluorescence emission, owing to stabilization of the excited state by the polar solvent molecules around the fluorescent molecule.[36] Finally, fluorescence quenching is another primary source of changes in fluorescence decay dynamics.

In a living cell, a large portion of NADH bind to a variety of enzymes and proteins in multistep metabolic pathways. When NADH binds to a large molecule, fluorescence lifetime and anisotropy will change significantly.[11,37] Free NADH signals can be differentiated from bound NADH based on their differences in temporal characteristics. Because 75 to 85% of intracellular fluid is water,[38] it is water molecules that mainly compose the solvent shell of free NADH. Thus it is reasonable to assume that the spectra of free NADH are the same both in aqueous solutions and in cells. According to the Stern-Volmer theory, fluorescence lifetime changes arising from quenching can be described by following equation,

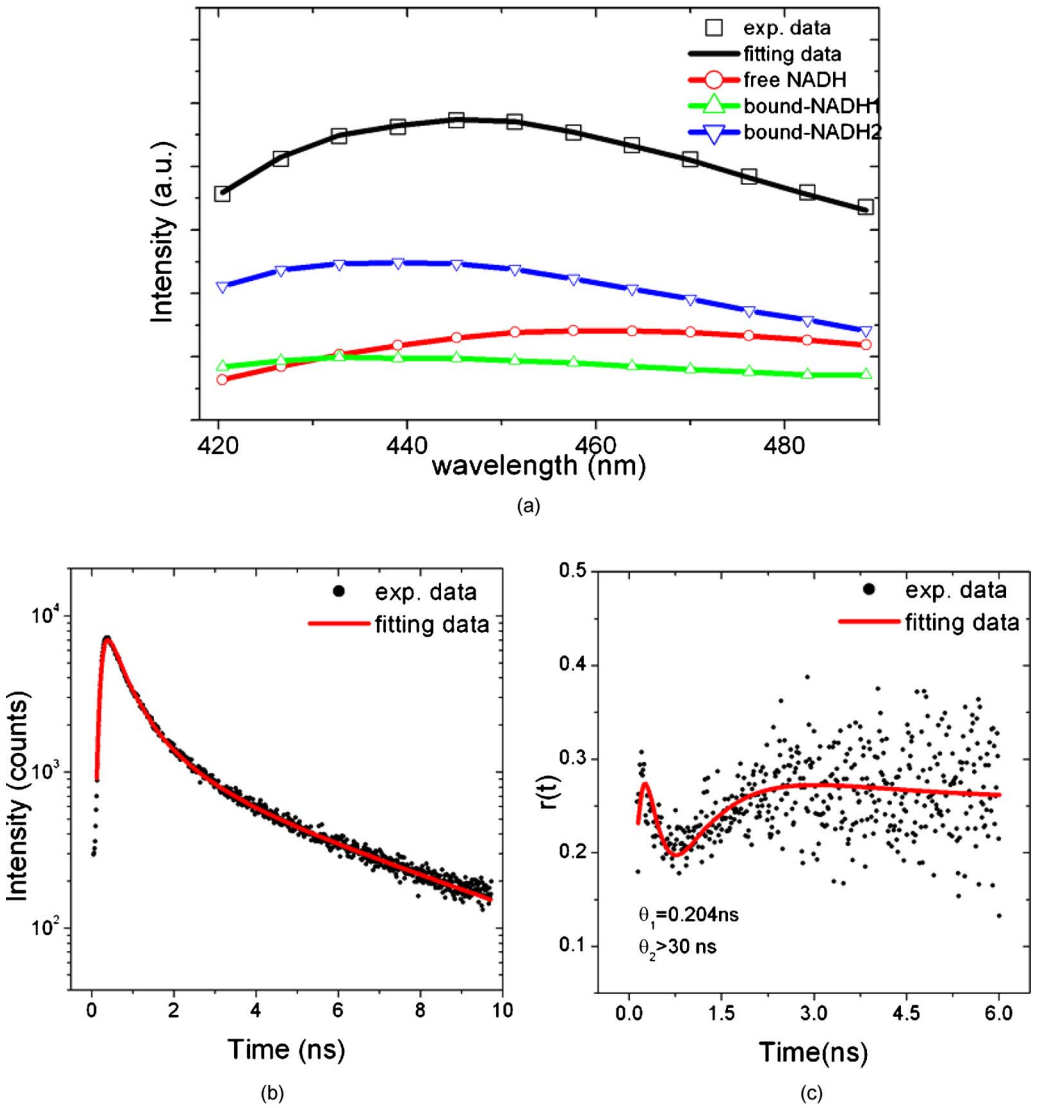

Fig. 4 Representative results of global fitting analysis of cellular NADH fluorescence signals from living SiHa cell samples. (a) The fluorescence spectra of the measured NADH signal, the fitted total signal, and the fractional decay associated spectra (DAS) of each component (free NADH, bound NADH1, and bound NADH2). (b) The measured and fitted fluorescence intensity decay. (c) The measured and fitted fluorescence associated anisotropy decay.

$$\frac{\tau_0}{\tau} = 1 + k_q \tau_0 [Q],$$

where τ_0 and τ are the fluorescence lifetimes in the absence and presence of quenchers, k_q is a bimolecular quenching constant and its typical value is about 1×10^{10} M^{-1} s^{-1}, and $[Q]$ is the concentration of the quencher.[20] Because averaged τ_0 of free NADH is short (only about 0.4 ns), theoretically it requires a 0.25-M concentration of quenchers to obviously change fluorescence lifetime. Few types of substances in cells can attain this concentration. For example, the concentration of oxygen, the primary fluorescence quencher,[20] is only about 0.032 mM in cells.[39] Therefore, the quenching of free NADH fluorescence would be negligible, and the fluorescence lifetime of free NADH in cells is assumed to be the same as in aqueous solution.

Therefore, similar to the analysis of the NADH and LDH mixture, the fluorescence intensity decay of NADH fluorescence from living cells was fitted by Eq. (7), where the first and second terms were the contributions from free and bound NADH, respectively. To minimize possible interference of the flavoprotein (FAD) fluorescence peaking around 530 nm,[22] only 12 short-wavelength channels from 420 to 490 nm were used in the global analysis. Representative results obtained from monolayer SiHa cell culture are shown in Fig. 4. As can be seen, excellent fittings to both the fluorescence spectrum and intensity decay were achieved. The spectral signal fitting showed that about three-quarters of total fluorescence intensity came from the bound NADH in living cells, and the spectral peaks of the bound NADH were blue shifted about 20 nm compared with the spectral peak of free NADH.

Table 1 Analysis of fluorescence intensity decays from cell samples. Maximal χ^2 value in all fittings was not more than 2. n is the number of cell samples, and five measurements were conducted from different sites in each sample. The free/bound values reflect the ratio of the fractional intensity defined in Eq. (4).

Samples		τ_1'(ns)	τ_2'(ns)	Free/bound	Changes
SiHa	Control (n=9)	1.15±0.07	4.63±0.11	0.45±0.02	—
	NaCN (n=7)	0.91±0.04	4.16±0.10	0.55±0.05	23%
	CCCP (n=8)	1.20±0.05	4.46±0.11	0.40±0.01	−11%
Ect1	Control (n=5)	1.14±0.05	4.98±0.21	0.32±0.05	—
	NaCN (n=5)	0.96±0.09	4.57±0.34	0.74±0.23	131%
	CCCP (n=4)	1.26±0.02	5.17±0.16	0.21±0.03	−34%

We conducted cellular-based measurements to exhibit the capabilities of our measurement system and global-fitting analysis. The results of all parameters obtained from SiHa and Ect1 cell samples before the treatments with a mitochondrial inhibitor and uncoupler are summarized in Table 1. SiHa cells are well-known ectocervical cancer cells, whereas the Ect1 cells are established from normal ectocervical epithelium immortalized by HPV-16 E6/E7 transformation.[40] As can be seen, the ratio of the fractional intensity of free NADH signal to bound NADH signal were 0.45 and 0.32 for SiHa cells and Ect1 cells, respectively. The Warburg hypothesis suggests that cancer cells mainly generate energy by anaerobic glycolysis, whereas normal cells mainly generate energy from oxidative phosphorylation. Since more types of enzymes participate in oxidative phosphorylation compared with glycolysis, there are more binding sites in oxidative phosphorylation.[37] This may provide an explanation why SiHa cells had a greater fraction of intracellular free NADH compared with Ect1 cells.

To further demonstrate the correlation of the ratio of free to bound NADH with the cell's metabolic state, the redox potential of cells were disturbed by the mitochondrial inhibitor NaCN and mitochondrial uncoupler CCCP, respectively.[4,5,28] The results of the cell samples after the treatments of NaCN and CCCP are also listed in Table 1. The values of free to bound NADH increased with NaCN treatment and decreased with CCCP treatment in both SiHa and Ect1 cells, which were consistent with previous studies.[4,5] However, the amplitudes of these changes were different. The changes in Ect1 cells were more significant compared with those in SiHa cells. For example, with NaCN treatment, the ratio increased by 23% in SiHa cells, whereas it increased by 131% in Ect1 cells. With CCCP treatment, the ratio decreased by three times more in Ect1 cells than in SiHa cells. Reasons for these differences between SiHa and Ect1 cells are currently undetermined. It should be noted that the measurement of FAD/NADH to estimate the redox state of cells was not evaluated in this study, because the signal of FAD fluorescence is extremely weak at the excitation wavelength of 360 nm.

To investigate viscosity of small solutes in cells, we analyzed the cellular fluorescence anisotropy decay of cell samples. Because NADH is a small molecule, the microviscosity for small molecules rather than the macroviscosity for large proteins or organelles could be probed by measuring NADH rotational mobility. A typical fluorescence anisotropy decay curve measured from a SiHa cell sample is shown in Fig. 4(c). Similar to the analysis of fluorescence anisotropy decay in the NADH and LDH mixture, the model based on Eq. (8) was used to fit the associated anisotropy decay. A typical fitting result for SiHa cells is shown together with the experimentally measured curve in Fig. 4(c). $r_{\lambda,1}'$ and $r_{\lambda,2}'$ were 0.36 and 0.25, respectively. θ_1 was 0.204 ns, and θ_2 was more than 30 ns. Again, the uncertain large θ_2 value meant that bound NADH in cells was rotationally immobile in the time scale of our measurement window, which was limited by the repetition rate (78 MHz) of our Ti:sapphire laser system and fluorescence lifetime of bound NADH.

The results of all measurements of SiHa and Ect1 cells before and after the treatments with NaCN and CCCP are listed in Table 2. As described before, the rotational diffusion time of free NADH θ_1 is proportional to the environmental viscosity. As a result, the cellular microviscosity could be calculated from the rotational diffusion time. Based on Stokes-Einstein equation $\theta_1 = \eta V/kT$, we found that the cellular microviscosity was about 1.6 times higher than water. This result is consistent with previous reports.[14,19] It should be pointed

Table 2 Analysis of associated anisotropy decays from cell samples. Maximal χ^2 value in all fittings was not more than 1.2. Viscosity was estimated from the rotational relaxation time of free NADH.

Samples		θ_1(ns)	θ_2(ns)	Viscosity (cP)
SiHa	Control (n=9)	0.206±0.003	>30	1.54±0.02
	NaCN (n=7)	0.187±0.010	>30	1.40±0.08
	CCCP (n=8)	0.209±0.002	>30	1.57±0.02
Ect1	Control (n=5)	0.202±0.004	>30	1.51±0.03
	NaCN (n=5)	0.166±0.027	>30	1.24±0.20
	CCCP (n=4)	0.206±0.001	>30	1.54±0.01

Table 3 Fitting results based on the same fluorescence signal from cells at single wavelengths of NADH fluorescence peaks. With the same measured fluorescence data, three sets of results were achieved, and $\chi^2=1.1$ for each fitting. Parameters in this table were defined in Eq. (6), and the fitting method was defined in Ref. 11.

	τ_1(ns)	a_1	τ_2(ns)	a_2	τ_3(ns)	a_3	τ_4(ns)	a_4
Fitting 1	0.10	0.39	0.39	0.46	1.54	0.17	6.50	0.05
Fitting 2	0.17	0.42	0.39	0.31	1.24	0.20	5.61	0.07
Fitting 3	0.16	0.43	0.35	0.27	0.97	0.23	4.63	0.09
	θ_1(ns)	r_{01}	θ_2(ns)	r_{02}	θ_3(ns)	r_{03}	θ_4(ns)	r_{04}
Fitting 1	0.18	0.27	0.53	0.32	7.36	0.30	23.8	0.40
Fitting 2	0.23	0.30	0.45	0.40	11.3	0.22	13.8	0.44
Fitting 3	0.88	0.15	0.51	0.43	9.48	0.25	33.9	0.34

out that the Stokes-Einstein equation holds only for spherically shaped molecules. Therefore, the values determined by this equation should be regarded as estimates. Furthermore, we found that the treatment with NaCN caused obvious decrease of the rotation diffusion time of free NADH, while the treatment with CCCP did not cause the same effect. It is known that NaCN interrupts the electron transport chain and causes hypoxia. Previous studies have demonstrated that hypoxia caused osmotic swelling of mitochondria.[41] A recent study based on real-time microscopy further pointed that the mitochondria of fibroblasts swelled when treated with rotenone or antimycin A, which caused hypoxia in cells, whereas the morphology of the mitochondria did not change when treated with CCCP.[42] The dilution of intramitochondrial fluid by swelling will reduce the viscosity in mitochondria, which are the sources of most of cellular NADH fluorescence.[23] These may explain the changes in the rotation diffusion time of free NADH when cells were treated with NaCN.

3.3 *Single Wavelength Fitting Versus Global Fitting Analyses*

In principle, the parameters in $I_{\lambda,c}(t)$ and $D_{\lambda,c}(t)$ models can be obtained by fitting the experimental curve recorded in a single wavelength band. However, this approach does not take advantage of the relationship between individual decay curves recorded in different wavelength bands to reduce the local minima and improve fitting accuracy. Global analysis facilitates the analysis of multiple measurements simultaneously in terms of internally consistent sets of fitting parameters. Previous study has demonstrated that global analysis can significantly improve accuracy compared with individual analysis.[43] In this study, we found that in the global fitting analysis, it was crucial to make use of the time-resolved fluorescence signals recorded from all 16 (12 for cells) emission wavelengths to effectively reduce multiple local minima and produce accurate fitting results. As an example, the cellular fluorescence measured at a single emission wavelength from controlled SiHa cells was fitted based on Eq. (6) using the method described in Ref. 11. As shown in Table 3, multiple minima were found, and three sets of parameters that produced the best fitting ($\chi^2=1.1$) were significantly different from each other, making it difficult to identify which set of parameters holds true physical meaning. However, the fitting results based on global analysis of 12 wavelengths presented in Tables 1 and 2 always converged to one single set of parameters. In addition, we also used the measurement result from the mixture solution of NADH and LDH to compare the fitting based on the signal at the single wavelength band, with the global fitting using signals recorded at 16 wavelength bands. As shown in Table 4, four sets of parameters that were significantly different from each other produced the best fitting ($\chi^2=1.2$), indicating that multiple local minima occurred in fitting the data from the mixture NADH solutions with simpler chemical composition in comparison with living cells. In contrast, the results based on global fitting converged to a single set of parameters again. These results demonstrated that global analysis provided more accurate fitting and physical meaning than the fitting based on a single wavelength band.

4 Conclusion

In this study, we develop a technique that simultaneously analyzes spectral and lifetime information of fluorescence signals. The fractions of intracellular free NADH and bound NADH are identified and further confirmed by their rotational diffusion abilities measured by the time-resolved fluorescence associated anisotropy. We find that the ratio of free to bound NADH fluorescence is sensitive to the cellular metabolism. It increases when the cells are treated with NaCN, a mitochondrial inhibitor, and decreases when cells are treated with CCCP, a mitochondrial uncoupler. Furthermore, the rotational mobility of free NADH is used to determine cellular microviscosity. The decrease in rotational diffusion time when the cells are treated with NaCN may be caused by the swelling of mitochondria. This time- and wavelength-resolved fluorescence based assay enhances our ability to develop a more accurate picture of NADH biochemistry and cellular energy metabolism *in vivo*. Previous study demonstrated that the NADH fluorescence measured from cell samples were dominated by signals from mitochondria.[23] The measured rotation diffusion time of free NADH mainly reflects the microviscos-

Table 4 Fitting results based on the same fluorescence signal from the NADH and LDH mixture solution at single wavelengths of NADH fluorescence peaks. With the same measured fluorescence data, four sets of results were achieved, and $\chi^2=1.2$ for each fittings. Parameters in this table were defined in Eq. (6), and the fitting method was defined in Ref. 11.

	τ_1(ns)	a_1	τ_2(ns)	a_2	τ_3(ns)	a_3	τ_4(ns)	a_4
Fitting 1	0.11	1.38	0.44	1.39	1.22	0.45	3.49	0.06
Fitting 2	0.09	1.44	0.41	1.47	1.10	0.48	2.91	0.09
Fitting 3	0.13	1.60	0.53	1.30	1.47	0.30	3.59	0.05
Fitting 4	0.16	1.68	0.58	1.11	1.24	0.24	2.71	0.11
	θ_1(ns)	r_{01}	θ_2(ns)	r_{02}	θ_3(ns)	r_{03}	θ_4(ns)	r_{04}
Fitting 1	0.13	0.45	0.17	0.33	13.68	0.31	11.01	0.55
Fitting 2	0.23	0.36	0.19	0.30	6.90	0.27	11.54	0.56
Fitting 3	0.17	0.27	0.19	0.35	7.24	0.47	20.41	0.45
Fitting 4	0.34	0.38	0.11	0.18	4.17	0.56	19.67	0.44

ity of intramitochondrial fluid. To measure the viscosity of fluids in mitochondria, cytoplasm, and nucleus, the analysis must be based on the NADH fluorescence signals measured from these cellular compartments, respectively. In principle, an imaging-guided spectroscopy method could be used to measure the viscosity in different cellular compartments.[23,44] However, the signals of cytosolic and nuclear compartments are very low because of much lower NADH concentration in comparison with the mitochondrial compartment. Further increase of excitation power or exposure time causes photobleaching of NADH in cells. In future studies, a two-photon excitation approach may be needed to reduce photobleaching. It should be noted that cellular measurements are based on SiHa and Ect1 cell lines before and after treatments with the mitochondrial inhibitor and uncoupler. In future studies, the control of cell metabolism will be extended to use serum starvation and hypoxia methods. More different cell lines will be used in future study to lead to more general results and conclusions.

Acknowledgments

We thank Zouyan Han, Xiaoju Tang, and Bo Zheng for the viscosity measurement of the NADH and LDH mixture. This work was supported by the Research Grants Council via grant HKUST618808.

References

1. B. Chance and G. R. Williams, "The respiratory chain and oxidative phosphorylation," *Adv. Enzymol. Relat. Subj. Biochem.* **17**, 65–134 (1956).
2. B. Chance, F. Jobsis, B. Schoener, and P. Cohen, "Intracellular oxidation—reduction states in vivo," *Science* **137**(3529), 499 (1962).
3. D. Williams, P. Lund, and H. A. Krebs, "Redox state of free nicotinamide-adenine dinucleotide in cytoplasm and mitochondria of rat liver," *Biochem. J.* **103**(2), 514 (1967).
4. D. K. Bird, L. Yan, K. M. Vrotsos, K. W. Eliceiri, E. M. Vaughan, P. J. Keely, J. G. White, and N. Ramanujam, "Metabolic mapping of MCF10A human breast cells via multiphoton fluorescence lifetime imaging of the coenzyme NADH," *Cancer Res.* **65**(19), 8766–8773 (2005).
5. Y. Wu, W. Zheng, and J. Y. Qu, "Sensing cell metabolism by time-resolved autofluorescence," *Opt. Lett.* **31**(21), 3122–3124 (2006).
6. P. M. Bayley and G. K. Radda, "Conformational changes and the regulation of glutamate-dehydrogenase activity," *Biochem. J.* **98**, 105–111 (1966).
7. J. M. Salmon, E. Kohen, P. Viallet, J. G. Hirschberg, A. W. Wouters, C. Kohen, and B. Thorell, "Microspectrofluorometric approach to the study of free bound Nad(p)h ratio as metabolic indicator in various cell-types," *Photochem. Photobiol.* **36**(5), 585–593 (1982).
8. J. R. Lakowicz, H. Szmacinski, K. Nowaczyk, and M. L. Johnson, "Fluorescence lifetime imaging of free and protein-bound Nadh," *Proc. Natl. Acad. Sci. U.S.A.* **89**(4), 1271–1275 (1992).
9. J. C. Brochon, P. Wahl, J. M. Jallon, and M. Iwatsubo, "Pulse fluorimetry study of beef-liver glutamate dehydrogenase-reduced nicotinamide adenine-dinucleotide phosphate complexes," *Biochemistry* **15**(15), 3259–3265 (1976).
10. A. Gafni and L. Brand, "Fluorescence decay studies of reduced nicotinamide adenine-dinucleotide in solution and bound to liver alcohol-dehydrogenase," *Biochemistry* **15**(15), 3165–3171 (1976).
11. H. D. Vishwasrao, A. A. Heikal, K. A. Kasischke, and W. W. Webb, "Conformational dependence of intracellular NADH on metabolic state revealed by associated fluorescence anisotropy," *J. Biol. Chem.* **280**(26), 25119–25126 (2005).
12. S. Balaz, "Modeling kinetics of subcellular disposition of chemicals," *Chem. Rec.* **109**(5), 1793–1899 (2009).
13. M. K. Kuimova, S. W. Botchway, A. W. Parker, M. Balaz, H. A. Collins, H. L. Anderson, and K. A. O. Suhling P. R., "Imaging intracellular viscosity of a single cell during photoinduced cell death," *Nat. Chem.* **1**, 69–73 (2009).
14. A. S. Verkman, "Solute and macromolecule diffusion in cellular aqueous compartments," *Trends Biochem. Sci.* **27**(1), 27–33 (2002).
15. P. A. Valberg and D. F. Albertini, "Cytoplasmic motions, rheology, and structure probed by a novel magnetic particle method," *J. Cell Biol.* **101**(1), 130–140 (1985).
16. A. D. Keith, W. Snipes, R. J. Mehlhorn, and T. Gunter, "Factors restricting diffusion of water-soluble spin labels," *Biochem. J.* **19**(3), 205–218 (1977).
17. H. P. Kao, J. R. Abney, and A. S. Verkman, "Determinants of the translational mobility of a small solute in cell cytoplasm," *J. Cell Biol.* **120**(1), 175–184 (1993).
18. E. Haustein and P. Schwille, "Ultrasensitive investigations of biological systems by fluorescence correlation spectroscopy," *Methods* **29**(2), 153–166 (2003).

19. K. Fushimi and A. S. Verkman, "Low viscosity in the aqueous domain of cell cytoplasm measured by picosecond polarization microfluorimetry," *J. Cell Biol.* **112**(4), 719–725 (1991).
20. J. R. Lakowicz, *Principles of Fluorescence Spectroscopy*, 2nd ed., Kluwer Academic, New York (1999).
21. Y. Wu and J. Y. Qu, "Autofluorescence spectroscopy of epithelial tissues," *J. Biomed. Opt.* **11**(5), 054023 (2006).
22. W. Zheng, Y. Wu, D. Li, and J. Y. Qu, "Autofluorescence of epithelial tissue: single-photon versus two-photon excitation," *J. Biomed. Opt.* **13**(5), 054010 (2008).
23. D. Li, W. Zheng, and J. Y. Qu, "Time-resolved spectroscopic imaging reveals the fundamentals of cellular NADH fluorescence," *Opt. Lett.* **33**(20), 2365–2367 (2008).
24. J. R. Taylor, M. C. Adams, and W. Sibbett, "Investigation of viscosity dependent fluorescence lifetime using a synchronously operated picosecond streak camera," *Appl. Phys.* **21**(1), 13–17 (1980).
25. P. A. A. De Beule, C. Dunsby, N. P. Galletly, G. W. Stamp, A. C. Chu, U. Anand, P. Anand, C. D. Benham, A. Naylor, and P. M. W. French, "A hyperspectral fluorescence lifetime probe for skin cancer diagnosis," *Rev. Sci. Instrum.* **78**(12), 123101 (2007).
26. D. Magde, R. Wong, and P. G. Seybold, "Fluorescence quantum yields and their relation to lifetimes of rhodamine 6G and fluorescein in nine solvents: Improved absolute standards for quantum yields," *Photochem. Photobiol.* **75**(4), 327–334 (2002).
27. Q. Y. Fang, T. Papaioannou, J. A. Jo, R. Vaitha, K. Shastry, and L. Marcu, "Time-domain laser-induced fluorescence spectroscopy apparatus for clinical diagnostics," *Rev. Sci. Instrum.* **75**(1), 151–162 (2004).
28. N. D. Kirkpatrick, C. P. Zou, M. A. Brewer, W. R. Brands, R. A. Drezek, and U. Utzinger, "Endogenous fluorescence spectroscopy of cell suspensions for chemopreventive drug monitoring," *Photochem. Photobiol.* **81**(1), 125–134 (2005).
29. J. M. Beechem, "Global analysis of biochemical and biophysical data," *Methods Enzymol.* **210**, 37–54 (1992).
30. M. E. Couprie, F. Merola, P. Tauc, D. Garzella, A. Delboulbe, T. Hara, and M. Billardon, "1st use of the UV super-aco free-electron laser—fluorescence decays and rotational-dynamics of the nadh coenzyme," *Rev. Sci. Instrum.* **65**(5), 1485–1495 (1994).
31. A. J. W. G. Visser and A. Vanhoek, "The fluorescence decay of reduced nicotinamides in aqueous-solution after excitation with a UV-mode locked ar ion laser," *Photochem. Photobiol.* **33**(1), 35–40 (1981).
32. B. Kierdaszuk, H. Malak, I. Gryczynski, P. Callis, and J. R. Lakowicz, "Fluorescence of reduced nicotinamides using one- and two-photon excitation," *Biophys. Chem.* **62**(1–3), 1–13 (1996).
33. S. V. Dabir, K. G. Tushar, H. L. P. Dasika, V. K. D. Nidamarty, and Y. R. Kalipatnapu, "Correlations and estimation of pureliquid viscosity," Chap. 4 in *Viscosity of Liquids: Theory, Estimation, Experiment, and Data*, D. S. Viswanath, Ed., pp. 135–405, Springer, Netherlands (2007).
34. J. T. Edward, "Molecular volumes and Stokes-Einstein equation," *J. Chem. Educ.* **47**(4), 261 (1970).
35. Z. Han, X. Tang, and B. Zheng, "A PDMS viscometer for microliter Newtonian fluid," *J. Micromech. Microeng.* **17**(9), 1828–1834 (2007).
36. B. Valeur, *Molecular Fluorescence: Principles and Applications*, Weinheim, New York (2002).
37. Y. Yuan, Y. Li, B. D. Cameron, and P. Relue, "Fluorescence anisotropy of cellular NADH as a tool to study different metabolic properties of human melanocytes and melanoma cells," *IEEE J. Sel. Top. Quantum Electron.* **13**(6), 1671–1679 (2007).
38. W. M. Becker, L. J. Kleinsmith, and J. Hardin, *The World of the Cell*, Benjamin, San Francisco (2003).
39. Y. Y. Lau, T. Abe, and A. G. Ewing, "Voltammetric measurement of oxygen in single neurons using platinized carbon ring electrodes," *Anal. Chem.* **64**(15), 1702–1705 (1992).
40. R. N. Fichorova, J. G. Rheinwald, and D. J. Anderson, "Generation of papillomavirus-immortalized cell lines from normal human ectocervical, endocervical, and vaginal epithelium that maintain expression of tissue-specific differentiation proteins," *Biol. Reprod.* **57**(4), 847–855 (1997).
41. G. Zahrebelski, A. L. Nieminen, K. Alghoul, T. Qian, B. Herman, and J. J. Lemasters, "Progression of subcellular changes during chemical hypoxia to cultured rat hepatocytes—a laser-scanning confocal microscopic study," *Hepatology (Philadelphia, PA, U. S.)* **21**(5), 1361–1372 (1995).
42. N. A. Pham, T. Richardson, J. Cameron, B. Chue, and B. H. Robinson, "Altered mitochondrial structure and motion dynamics in living cells with energy metabolism defects revealed by real time microscope imaging," *Microsc. Microanal.* **10**(2), 247–260 (2004).
43. J. R. Knutson, J. M. Beechem, and L. Brand, "Simultaneous analysis of multiple fluorescence decay curves—a global approach," *Chem. Phys. Lett.* **102**(6), 501–507 (1983).
44. C. E. Bigelow, D. L. Conover, and T. H. Foster, "Confocal fluorescence spectroscopy and anisotropy imaging system," *Opt. Lett.* **28**(9), 695–697 (2003).